TABLE I. Excitation (γ_{12}, left column) and de-excitation (γ_{21}, right column) rates for NPIs between the ground state and first excited state of a ^{188}Os nucleus for different temperatures and densities, calculated using the ISOMEX code [25].

Density	$\mathcal{T} = 0.01$ MeV	$\mathcal{T} = 0.1$ MeV	$\mathcal{T} = 1$ MeV
10 g/cm^3	$6.0 \cdot 10^2$ / $6.5 \cdot 10^8 s^{-1}$	$7.3 \cdot 10^8$ / $6.9 \cdot 10^8 s^{-1}$	$1.6 \cdot 10^{10}$ / $3.8 \cdot 10^9 s^{-1}$
10^3 g/cm^3	$7.0 \cdot 10^2$ / $7.6 \cdot 10^8 s^{-1}$	$7.3 \cdot 10^8$ / $6.9 \cdot 10^8 s^{-1}$	$1.6 \cdot 10^{10}$ / $3.8 \cdot 10^9 s^{-1}$
10^5 g/cm^3	$8.0 \cdot 10^2$ / $8.6 \cdot 10^8 s^{-1}$	$7.8 \cdot 10^8$ / $7.3 \cdot 10^8 s^{-1}$	$1.6 \cdot 10^{10}$ / $3.8 \cdot 10^9 s^{-1}$

check that the results converge [18]. This serves as verification of the method and a baseline that allows us to evaluate the thermal effects of the plasma.
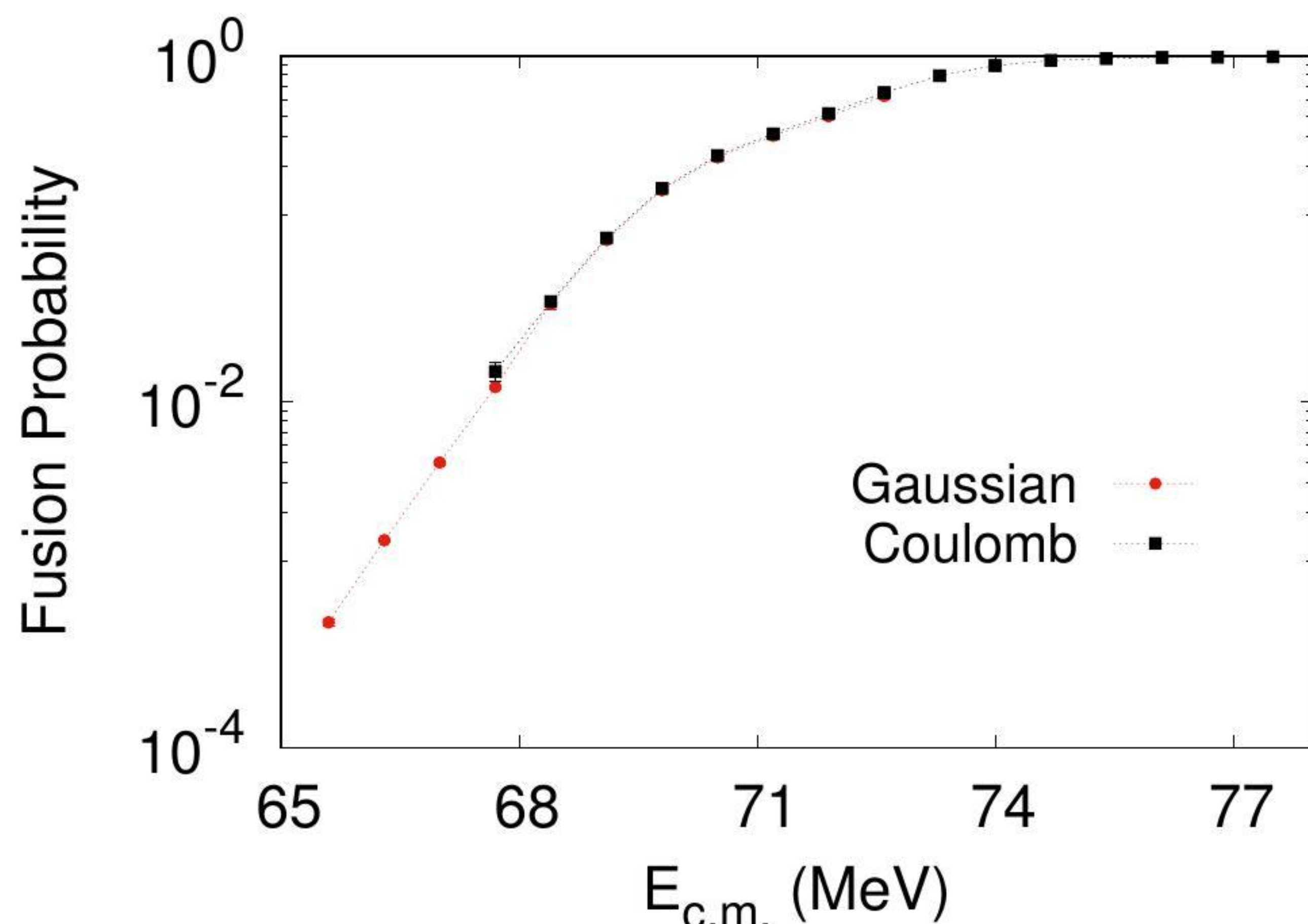

FIG. 1. A construction of the energy-resolved fusion probability for a ^{16}O projectile and ^{188}Os target with coupled channels but without a plasma environment ($\mathcal{T} = 0$ MeV). Gaussian and Coulomb wave packets are used, taking the average energy-resolved fusion probability for a range of incident mean energies, E_0. Error bars due to statistical error are included but most are insignificant. The nominal Coulomb barrier between these nuclei is 71.7 MeV.

Fig. 2 shows the population of the radial grid basis states over time for an initial Gaussian wave packet with an average energy $E_0 = 70$ MeV and a temperature $\mathcal{T} = 0.1$ MeV. The change of population of both the ground state (elastic channel) and the 2^+ excited state of ^{188}Os (inelastic channel) due to both thermal effects and the radial coupling between these states can be observed.

To isolate the effects of temperature on fusion probability, the increase in energy-resolved fusion probability was calculated using the ratio between coupled channels calculations at either $\mathcal{T} = 0.1$ MeV or $\mathcal{T} = 0.5$ MeV and $\mathcal{T} = 0$ MeV, shown in Fig. 3. The fusion probability was calculated by taking the average energy-resolved fusion probability for initial wave packets with varying E_0. For $\mathcal{T} = 0.1$ MeV, the green (square) points were calculated using a Gaussian wave packet with $E_0 = 60$, 63, 65, 67 and 70 MeV, and the blue (circle) points were calculated using a Coulomb wave packet with $E_0 = 65$, 67 and 70 MeV. The same method was used for both
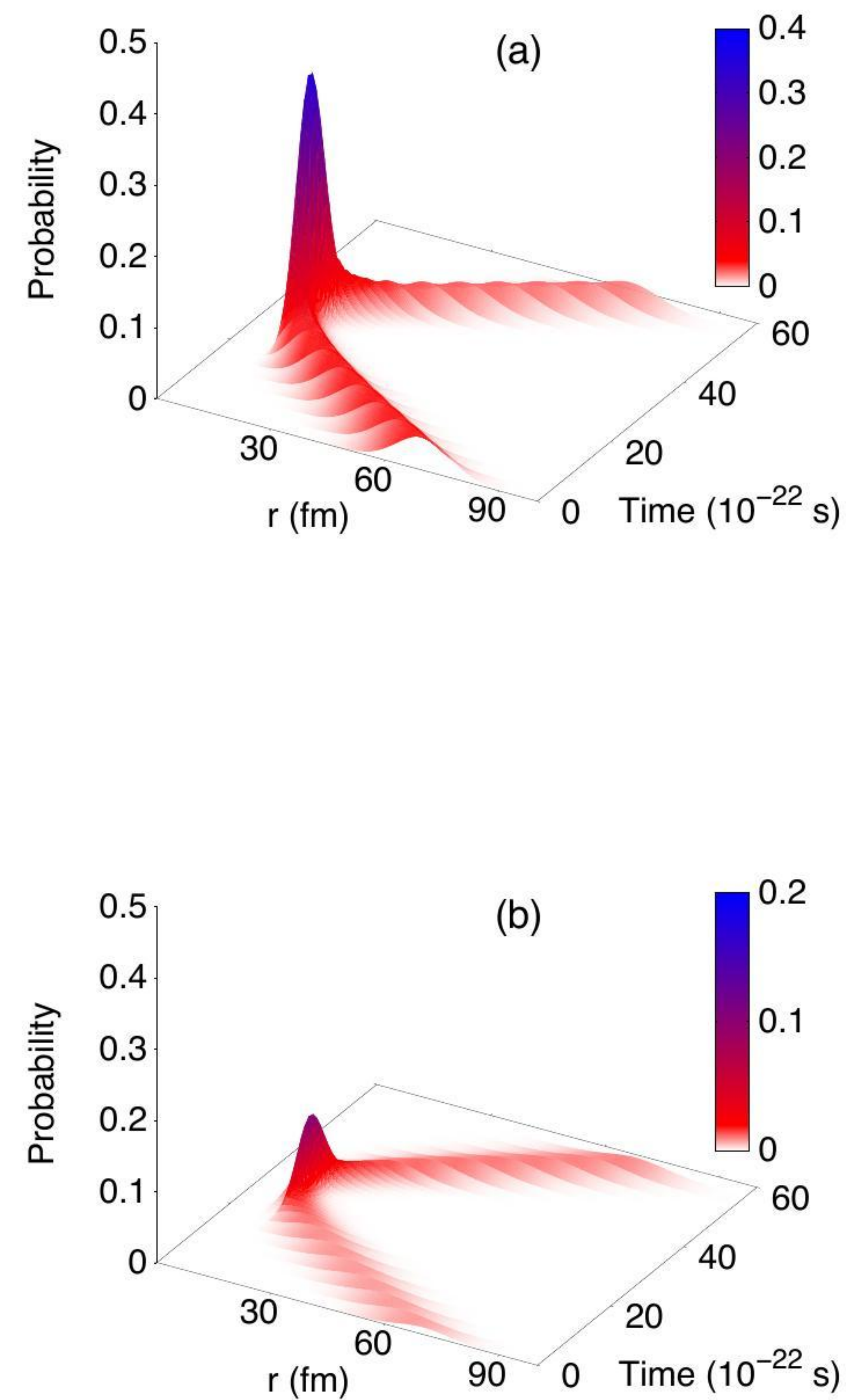

FIG. 2. Radial position probability as a function of internuclear radius and time for a head-on collision of ^{16}O + ^{188}Os with $E_0 = 70$ MeV and $\mathcal{T} = 0.1$ MeV. The radial probability changes for (a) the elastic and (b) inelastic channels respectively, as the nuclei approach their Coulomb barrier ($r \approx 11.5$ fm). The inelastic channel is thermally populated before the target and projectile interact with each other. For visualisation, when the mean radius is larger than 20 fm, the time step is 3×10^{-22} s.

$\mathcal{T} = 0$ and $\mathcal{T} = 0.5$ MeV. The error bars associated with these points are simply due to the standard error in the mean. We use a Gaussian wave packet for its accuracy at deep sub-barrier energies compared to a Coulomb wave packet. However, a Coulomb wave packet offers a better global description of fusion probability around and above